A complete modelling of the series-resonant converter in ZCS mode

Hubert Piquet, Yvon Chéron, Patrick Kuo-Peng

A COMPLETE MODELLING OF THE SERIES-RESONANT CONVERTER IN Z.C.S. MODE

P. Kuo-peng, Y. Chéron and H. Piquet.

Laboratoire d'Electrotechnique et d'Electronique Industrielle, France.

Abstract. In most cases, the series-resonant converter is equipped with snubbers to reduce switching losses. These auxiliary circuits, which lead to an increase of the circuit order, also fundamentally modify the operation and the characteristics of the series-resonant converter.
This paper presents a complete modelling of non-reversible series-resonant converters operating in thyristor mode (Z.C.S.) equipped with snubbers both on the inverter side (inductors) and on the rectifier side (capacitors). Based on the representation of the state plane, this analytical study characterizes the steady state operation of the converter and determines the main component stresses. The results of these analytical studies are integrated into a software which constitutes a powerful tool to design the converter.

Keywords. Series-resonant converter, modelling, snubbers, state-plane.

In the numerous bibliography about series-resonant converter (1-5), the snubbers are usually neglected or taken into account in an incomplete manner (6). After the presentation of the complete study of this converter in Z.V.S. mode (5), this paper focuses on the converter operation in Z.C.S. mode. The structure of this converter is indicated in Fig.1. It is mainly composed of a voltage inverter and a diode rectifier connected through a resonant circuit and a transformer. The inverter requires turn-on controlled switches which turn-off spontaneously at the current zero-crossing. These switches, which can be effectively some thyristors in high power and low frequency applications are represented by thyristors. In order to reduce switching losses, inductors are series-connected with the switches of the inverter and capacitors are connected in parallel manner across the diodes of the rectifier. These capacitors also can represent the parasitic capacitance of the secondary winding of the transformer.

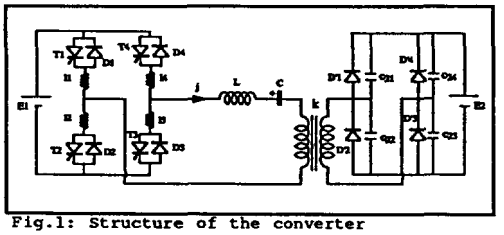

Fig.1: Structure of the converter

NOTATION. NORMALIZED QUANTITIES

- C resonant capacitor,
- L resonant inductor,
- l_j snubber inductor of the inverter,
- C_{2j} snubber capacitor of the rectifier,
- ℓ equivalent inductor representing the snubbers of the inverter during its commutation,
- C_2 equivalent capacitor representing the snubbers of the rectifier during its commutation,
- f_0 natural frequency of the resonant circuit,
- f_s frequency operation,
- E_1 input voltage,
- E_2 output voltage,
- j current in the resonant circuit,
- I_2 DC output current,
- v_c voltage across the resonant capacitor,
- k turns ratio of the transformer.

In addition to these notations, the various analytic studies of the series-resonant converter exposed in this paper use the following normalized units :

$y = \dfrac{j}{E_1\sqrt{\dfrac{C}{L+\ell}}}$ normalized current in the resonant circuit

$Y_{avg} = \dfrac{kI_2}{E_1\sqrt{\dfrac{C}{L+\ell}}}$ normalized average load current,

$x = \dfrac{v_c}{E_1}$ normalized voltage across the capacitor C,

$q = \dfrac{E_2}{kE_1}$ normalized load voltage,

$a_\ell = \dfrac{\ell}{L}$ normalized snubber inductor of the inverter,

$a_2 = \dfrac{k^2C_2}{C}$ normalized snubber capacitor of the rectifier,

$u = \dfrac{f_s}{f_0}$ normalized frequency of operation.

with

$$f_0 = \frac{1}{2\pi\sqrt{(L+\ell)C}}$$

This system of base units leads to the derivation of dimensionless equations that characterize a structure instead of a particular circuit.
In this paper, Function Atan2(x) is the function Arctg(x) with value lying between 0 and π.

ASSUMPTIONS

The study of the converter is carried out under the following assumptions :

- the transformer is ideal and has a 1:1 ratio,
- the switches are ideal in that they commutate instantaneously,
- the DC voltages is supposed perfect,
- the losses in the passive components are negligible.

STUDYING METHOD

Under these assumptions, the study of the series-resonant converter reduces to the study of the response of a series-resonant network connected on one side to a voltage source $V_1 = \pm E_1$ of frequency f_s and on the other side to a voltage source $v_2 = \pm E_2$ in phase with the current in the resonant circuit. This study is greatly facilitated by using the state plane representation (2 and 3). This analytico-graphical method, based on an exact graphical representation for steady state as well as transiently, avoids writing time equations of the system and allows straight deduction of the relations which characterize the operation of mode being studied.

However, taking the snubbers of the converter into account, specially the snubber of the rectifier, leads to characterize three modes of operation :
- Normal operation, characterized by the fact that the thyristors are turned-on after the end of the rectifier commutation. Short-circuit operation is a particular case of the normal operation.
- secondary operation, characterized by the fact that the rectifier commutation ends after the inverter commutation has been completed. No-load operation is a particular case of the secondary operation.
- criss-cross region of operation in which the rectifier commutation ends during the commutation of the inverter.

In that case, the state plane analysis is possible, though only the quantities related to a single resonant network can be drawn in the same state plane. Thus in order to carry out this study, several state planes should be used, one to show the operation between commutations and the others to represent the commutations. Nevertheless, it will be shown that it is possible to determine appropriate formula allowing the passage from one state plane to the other one.

In this paper, owing to the symmetry of the operation of the converter, only the positive half-wave of the current is represented in the state plane.

MODELLING THE SERIES-RESONANT CONVERTER IN Z.C.S. MODE

The structure of the converter is indicated in Fig.1. Let :

$$l_1 = l_2 = l_3 = l_4 = \frac{\ell}{2} \quad (1)$$

$$C_2 = C_{21} = C_{22} = C_{23} = C_{24} \quad (2)$$

$$k_\ell = \sqrt{\frac{2 + a\ell}{2 + 2a\ell}} \quad (3)$$

$$k_2 = \sqrt{1 + \frac{1}{a_2}} \quad (4)$$

$$G_2 = \frac{C_2 C}{C_2 + C} \quad (5)$$

Normal operation

Representation in the state plane. The normal operation is characterized by the series of modes indicated in Fig.2. Let :

$$Y_\ell = \frac{j}{E_1}\sqrt{\frac{(L+\ell)}{C}} \quad (6)$$

$$X_\ell = X^* = \frac{V_c}{E_1} \quad (7)$$

$$Y^* = \frac{j}{E_1}\sqrt{\frac{(L+\frac{\ell}{2})}{C}} \quad (8)$$

$$X^* = \frac{V_{c2}}{E_1} \quad (9)$$

$$Y^* = \frac{j}{E_1}\sqrt{\frac{(L+\ell)}{G_2}} \quad (10)$$

Mode 1, represents the commutation of the rectifier. It is initiated by the zero crossing of the current in the resonant network. This mode takes end when the capacitor C_2 is reverse biased. Mode 3 corresponds to the commutation of the inverter and it is initiated by the control signal. This mode ends at the zero crossing of the current in the inverter diodes.

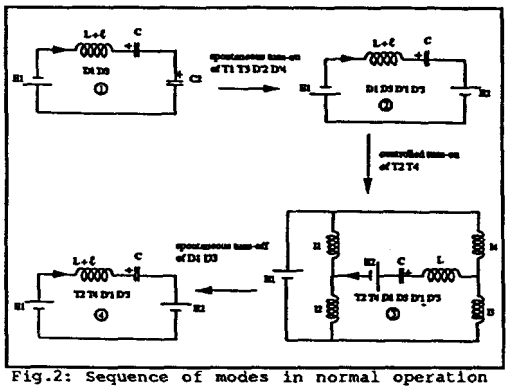

Fig.2: Sequence of modes in normal operation

According to Thevenin's theorem, equivalent circuit representing the commutation of the inverter (modes 3) can be reduce to a second order circuit.
Taking the previous remarks into account, the state plane of the normal operation is shown in Fig.3.

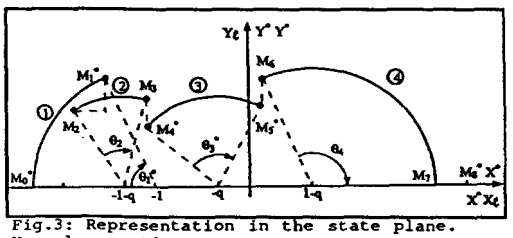

Fig.3: Representation in the state plane. Normal operation

θ_1^* and θ_3^* are respectively the normalized commutation times of the rectifier and of the inverter.
θ_1^*, θ_2 and θ_3^* correspond to the conduction times of the inverter diodes ; θ_3^* and θ_4, those of the thyristors.

The transformation rules allowing the passage from the state plane (X^*, Y^*) to the state plane (X_ℓ, Y_ℓ) are given by the following equations:
before the commutation of the rectifier

$$X^* = X_\ell - q \quad (11)$$

$$Y^* = k_2 Y_\ell \quad (12)$$

after the commutation of the rectifier

$$X^* = X_\ell + q \quad (13)$$

$$Y^* = k_2 Y_\ell \quad (14)$$

and those between the state plane (X_ℓ, Y_ℓ) and the state plane (X^*, Y^*) are given by :

$$X^* = X_\ell \quad (15)$$

$$Y^* = k_\ell Y_\ell \quad (16)$$

The discontinuous conduction mode occurs when the point M_3 of the state plane (Fig.3) is located on X-axis. During this mode, voltage v_c and current j are frozen until the triggering of the thyristors.

State plane analysis. The key relationships that fully determine the state plane trajectories are :

$$(X_0^*+1)^2 = (X_1^*+1)^2+Y_1^{*2} \quad (17)$$

$$(X_2+1+q)^2+Y_2^2 = (X_3+1+q)^2+Y_3^2 \quad (18)$$

$$(X_4^*+q)^2+Y_4^{*2} = (X_5^*+q)^2+Y_5^{*2} \quad (19)$$

$$(X_6-1+q)^2+Y_6^2 = (X_7-1+q)^2 \quad (20)$$

The voltage variation across the capacitor G_2 during the commutation of the rectifier is given by :

$$X_1^*-X_0^* = 2q(1+a_2) \quad (21)$$

Relations (11) to (21) enable to write all the coordinates in fonction of q, X_m, a_2, θ_2 and θ_3^* :

$$X_0^* = -X_m-q \quad (22)$$

$$X_1^* = q(1+2a_2)-X_m \quad (23)$$

$$Y_1^{*2} = 4q(1+a_2)(X_m-qa_2-1) \quad (24)$$

$$X_2 = 2qa_2-X_m \quad (25)$$

$$Y_2^2 = 4qa_2(X_m-qa_2-1) \quad (26)$$

$$X_3=X_4^*= -1-q+(X_2+q+1)\cos\theta_2+Y_2\sin\theta_2 \quad (27)$$

$$Y_3 = -(X_2+q+1)\sin\theta_2 +Y_2\cos\theta_2 \quad (28)$$

$$Y_4^* = k_\ell Y_3 \quad (29)$$

$$X_5^*= X_6 = -q+(X_4^*+q)\cos\theta_3^*+Y_4^*\sin\theta_3^* \quad (30)$$

$$Y_5^* = -(X_4^*+q)\sin\theta_3^*+Y_4^*\cos\theta_3^* \quad (31)$$

$$Y_6 = \frac{Y_5^*}{k_\ell} \quad (32)$$

Angle θ_2 is incremented until the steady state operation is reached ($X_7 = X_m$). Commutation angle θ_3^* is calculated at the current zero-crossing of the inverter's diodes.
The flowchart indicated in Fig.6a, summarizes the calculation method of all the coordinates of the state plane shown in Fig.3.

The normalized frequency of operation is defined by:

$$u = \frac{\pi}{\frac{\theta_1^*}{k_2}+\theta_2+k_\ell\theta_3^*+\theta_4} \quad (33)$$

where

$$\theta_1^* = \pi - \mathrm{Atan2}\left(\frac{Y_1^*}{X_1^*+1}\right) \quad (34)$$

$$\theta_4 = \mathrm{Atan2}\left(\frac{Y_6}{X_6-1+q}\right) \quad (35)$$

θ_2 and θ_3^* are numerically calculated according to the method presented in Fig.6a.

The normalized average load current is given by :

$$Y_{avg} = \frac{2u(X_m-qa_2)}{\pi} \quad (36)$$

Normal operation limits. Mathematical relations (17) to (36) enable us to study the normal operation in steady state of the converter. However it is necessary to define their application ranges corresponding to the sequence of modes shown in Fig.4 and defined by the following relations :

$$X_0^* \le X_1^* \quad (37)$$

$$Y_3 \ge 0 \quad (38)$$

$$X_2 \le X_3 \quad (39)$$

The equality of relations (37) and (38) correspond respectively to the short-circuit operation of the converter and to the boundaries locus of the critical operation (limit between continuous and discontinuous conduction modes of operation of the converter) . These relations can be expressed as functions of q, X_m, and a_2 :

$$q = 0 \quad (40)$$

$$X_m = \frac{q^2a_2+2q-2}{q-1} \quad (41)$$

The equality of relation (39) represents the boundaries locus of the normal operation. This constraint is calculated numerically.

An exemple of the operating area of the converter in the plane $q(X_m)$ is shown in Fig.9.

Secondary operation

Representation in the state plane. The secondary operation is represented by the sequence of modes indicated in Fig.4. In addition to relations (6) to (10) let :

$$Y^{**} = \frac{j}{E_1}\sqrt{\frac{(L+\frac{\ell}{2})}{G_2}} \quad (42)$$

$$X^{**} = \frac{v_{G_2}}{E_1} \quad (43)$$

Mode 2 represents the commutation of the inverter and it is initiated by the control signal which is triggered before the end of the commutation of the rectifier (modes 1, 2 and 3).

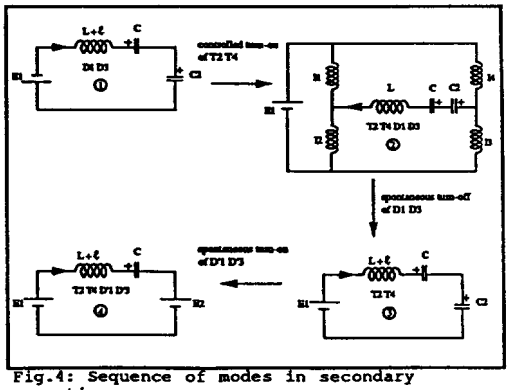

Fig.4: Sequence of modes in secondary operation

In the light of remarks made in the foregoing paragraph, the secondary operation can be drawn in the state plane (Fig.5).

θ_1^* and θ_2^{**} are the conduction angles of the inverter diodes, and θ_2^{**}, θ_3^* and θ_4, those of the thyristors. θ_1^*, θ_2^{**} and θ_3^* correspond to the commutation angles of the rectifier, and θ_2^{**}, that of the inverter.

The transformation rules allowing the passage from the state plane (X^*, Y^*) to the state plane (X_ℓ, Y_ℓ) are given by the relations (11) to (14) and those between the state plane (X^{**}, Y^{**}) and state plane (X^*, Y^*) are given by

$$X^{**} = X^{*} \quad (44)$$

$$Y^{**} = k_\ell Y^{*} \quad (45)$$

The discontinuous conduction mode occurs when the point M_1^{*} (Fig.5) is located on X-axis.

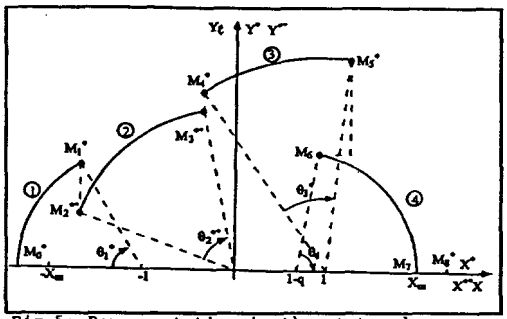

Fig.5: Representation in the state plane. Secondary operation

State plane analysis. The main relations that enable us to determine the whole trajectory in the state plane are :

$$(X_0^{*}+1)^2 = (X_1^{*}+1)^2+Y_1^{*2} \quad (46)$$

$$X_2^{**2}+Y_2^{**2} = X_3^{**2}+Y_3^{**2} \quad (47)$$

$$(X_4^{*}-1)^2+Y_4^{*2} = (X_5^{*}-1)^2+Y_5^{*2} \quad (48)$$

$$(X_6-1+q)^2+Y_6^2 = (X_7-1+q)^2 \quad (49)$$

The voltage variation across the capacitor G_2 during the commutation of the rectifier is given by :

$$X_5^{*}-X_0^{*} = 2q(1+a_2) \quad (50)$$

Relations (44) to (50) enable to write all the coordinates in fonction of q, X_m, a_2, θ_1^{*} and θ_2^{**} :

$$X_0^{*} = -X_m-q \quad (51)$$

$$X_1^{*} = X_2^{**} = -1+(1-q-X_m)\cos\theta_1^{*} \quad (52)$$

$$Y_1^{*2} = (-1+q+X_m)\sin\theta_1^{*} \quad (53)$$

$$Y_2^{**} = k_\ell Y_1^{*} \quad (54)$$

$$X_3^{**} = X_4^{*} = X_2^{**}\cos\theta_2^{**}+Y_2^{**}\sin\theta_2^{**} \quad (55)$$

$$Y_3^{**} = Y_2^{**}\cos\theta_2^{**}-X_2^{**}\sin\theta_2^{**} \quad (56)$$

$$Y_4^{*} = \frac{Y_3^{**}}{k_\ell} \quad (57)$$

$$X_5^{*} = q(1+2a_2)-X_m \quad (58)$$

$$Y_5^{*2} = (X_4^{*}-1)^2+Y_4^{*2}-(X_5^{*}-1)^2 \quad (59)$$

$$X_6 = X_5^{*}-q \quad (60)$$

$$Y_6 = \frac{Y_5^{*}}{k_2} \quad (61)$$

θ_1^{*} is incremented until the steady state operation is reached ($X_7 = X_m$). Commutation angle θ_2^{**} is calculated at the current zero-crossing of the inverter's diodes.

The flowchart indicated in Fig.6b, summarizes the calculation method of all the coordinates of the state plane shown in Fig.5.

The normalized frequency of operation is defined by:

$$u = \frac{\pi}{\frac{\theta_1^{*}}{k_2}+\frac{k_\ell\theta_2^{**}}{k_2}+\frac{\theta_3^{*}}{k_2}+\theta_4} \quad (62)$$

where

$$\theta_3^{*} = \text{Atan2}\left(\frac{Y_4^{*}}{X_4^{*}-1}\right) - \text{Atan2}\left(\frac{Y_5^{*}}{X_5^{*}-1}\right) \quad (63)$$

$$\theta_4 = \text{Atan2}\left(\frac{Y_6}{X_6-1+q}\right) \quad (64)$$

θ_1^{*} and θ_2^{**} are numerically calculated according to the method presented in Fig.6b. The normalized average load current is always given by relation (36).

Secondary operation limits. As for the normal operation, the application field of the mathematical relations above-stated must be defined and therefore, the following relations have to be checked :

$$X_0^{*} \le X_1^{*} \quad (65)$$

$$Y_1^{*} \ge 0 \quad (66)$$

$$X_4^{*} \le X_5^{*} \quad (67)$$

$$X_6 \le X_7 \quad (68)$$

Relations (65) to (67) respectively mean that the thyristors are triggered after the current zero crossing in the resonant tank, that the converter is in a continuous conduction mode, and that the rectifier ends its commutation after the inverter one. The equality of relation (68) reflects the no load-operation of the converter. The limit loci associated with Eqs. (65), (66) and (68) are respectively defined by :

$$X_m = \frac{q^2a_2}{q-1} \quad (69)$$

$$X_m = \frac{-k_2^2q^2a_2+2q-2}{k_2^2(1-q)-2} \quad (70)$$

$$X_m = qa_2 \quad (71)$$

The equality of relation (67) is calculated numerically.

An exemple of the operating area of the converter in the plane q(Xm) is shown in Fig.9.

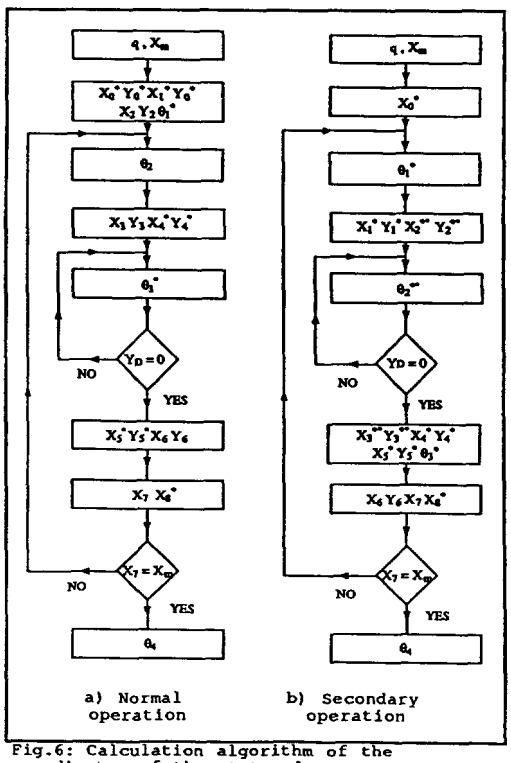

Fig.6: Calculation algorithm of the coordinates of the state plane

Criss-cross region of operation

Representation in the state plane. The criss-cross region of operation is characterized by the fact that the rectifier commutation ends during the inverter one. The equivalent circuits of each sequence is indicated in Fig.7. Sequences 1 and 2, correspond to the commutation of the rectifier, and sequences 2 and 3, those of the inverter.

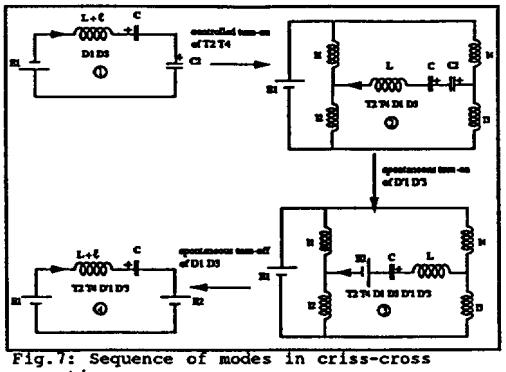

Fig.7: Sequence of modes in criss-cross operation

As for the other operations, the criss-cross operation is drawn in several state planes (Fig.8).
The transformation rules allowing the passage from the state plane (X^{**},Y^{**}) to the state plane (X^{*},Y^{*}) are given by (44) and (45), those between the state plane (X^{*},Y^{*}) and the state plane (X_ℓ,Y_ℓ) are given by relations (11) to (14), those between the state plane (X_ℓ,Y_ℓ) and the state plane (X^{*},Y^{*}) are given by (15) and (16) and finally, those between the state plane (X^{**},Y^{**}) and the state plane (X^{*},Y^{*}) are given by :

$$X^{**} = X^{*}+q \tag{72}$$

$$Y^{**} = k_2 Y^{*} \tag{73}$$

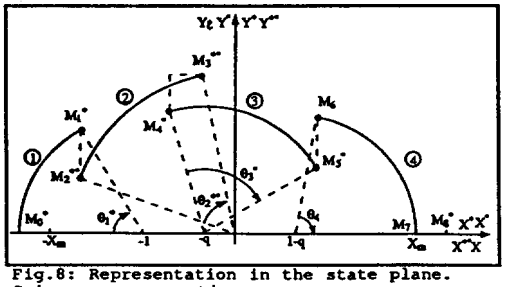

Fig.8: Representation in the state plane. Criss-cross operation

θ_1^{*}, θ_2^{**} and θ_3^{*} are the conduction angles of the inverter diodes, and θ_2^{**}, θ_3^{*} and θ_4, those of the thyristors. θ_2^{**} and θ_1^{*} correspond to the commutation angle of the rectifier, and θ_2^{**} and θ_3^{*} those of the inverter.

State plane analysis. The trajectory in the state plane is completely determined by the following main relations :

$$(X_0^{*}+1)^2 = (X_1^{*}+1)^2+Y_1^{*2} \tag{74}$$

$$X_2^{**2}+Y_2^{**2} = X_3^{**2}+Y_3^{**2} \tag{75}$$

$$(X_4^{*}+q)^2+Y_4^{*2} = (X_5^{*}+q)^2+Y_5^{*2} \tag{76}$$

$$(X_6-1+q)^2+Y_6^2 = (X_7-1+q)^2 \tag{77}$$

The transformation rules between state planes above-stated and relations (74) to (77) enable to write all the coordinates of the state plane in function of X_m, q, θ_1^{*}, θ_2^{**} and θ_3^{*} :

$$X_0^{*} = -X_m-q \tag{78}$$

$$X_1^{*} = X_2^{**} = -1+(1-q-X_m)\cos\theta_1^{*} \tag{79}$$

$$Y_1^{*2} = (-1+q+X_m)\sin\theta_1^{*} \tag{80}$$

$$Y_2^{**} = k_\ell Y_1^{*} \tag{81}$$

$$X_3^{**} = X_2^{**}\cos\theta_2^{**}+Y_2^{**}\sin\theta_2^{**} \tag{82}$$

$$Y_3^{**} = Y_2^{**}\cos\theta_2^{**}-X_2^{**}\sin\theta_2^{**} \tag{83}$$

$$X_4^{*} = X_3^{**}-q \tag{84}$$

$$Y_4^{*} = \frac{Y_3^{**}}{k_\ell} \tag{85}$$

$$X_5^{*} = X_6 = -q+(X_4^{*}+q)\cos\theta_3^{*}+Y_4^{*}\sin\theta_3^{*} \tag{86}$$

$$Y_5^{*} = -(X_4^{*}+q)\sin\theta_3^{*}+Y_4^{*}\cos\theta_3^{*} \tag{87}$$

$$Y_6 = \frac{Y_5^{*}}{k_2} \tag{88}$$

θ_1^{*} is incremented until the steady state operation is reached ($X_7 = X_m$). Commutation angle θ_2^{**}, is calculated when the capacitor c_2 voltage becomes equal to the DC output voltage q. θ_3^{*} is calculated at the current zero-crossing of the inverter diodes.
The flowchart indicated in Fig.10, summarizes the calculation method of all the coordinates of the state plane shown in Fig.8.

The normalized frequency of operation is defined by:

$$u = \frac{\pi}{\frac{\theta_1^{*}}{k_2}+\frac{k_\ell\theta_2^{**}}{k_2}+k_\ell\theta_3^{*}+\theta_4} \tag{89}$$

where

$$\theta_4 = \mathrm{Atan2}\left(\frac{Y_6}{X_6-1+q}\right) \tag{90}$$

θ_1^{*}, θ_2^{**} and θ_3^{*} are numerically calculated according to the method presented in Fig.10. The normalized average load current is always given by relation (36).

Criss-cross operation limits. In the $q(X_m)$ plane (Fig.9), the area where this type of operation takes place is determined on the one hand by the previous analysis and on the other hand by the following relation :

$$X_1^{*} \geq X_0^{*} \tag{91}$$

This relation means that the thyristors must be triggered after the curent zero-crossing in the resonant tank.

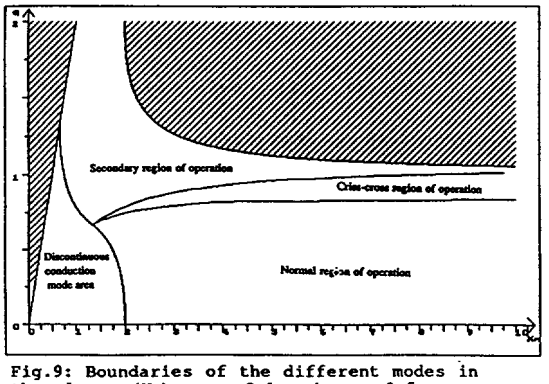

Fig.9: Boundaries of the different modes in the plane $q(X_m)$. a_ℓ = 0.1 and a_2 = 0.5

PRESENTATION OF THE SOFTWARE

The results of these analytical studies are integrated into a software which is able to plot the characteristics of the converter with or without snubbers on the inverter and/or on the rectifier, as:
- DC output voltage versus average load current at a constant frequency (Fig.11) or at a constant delay angle between the turn-on control and the current zero-crossing (Fig.12), or DC output voltage versus frequency at a constant load resistance (Fig.13),
- any electric quantity versus a second one at a constant output voltage (Fig.16). These electric quantities can be :
• the frequency of operation,
* the delay angle between the turn-on control of the thyristors and the current zero crossing in the resonant tank,
* the maximun voltage across the resonant capacitor,
* the peak current in the resonant tank,
* the current in the resonant circuit when the thyristor is turned-on,
• the current in the resonant circuit when the inverter's diode is turned-off,
• di/dt in the thyristor when it is turned-on.

These quantities are not exhaustive, because they are all accessible from the analysis of the state plane.

The limit of the hatched region of the diagram (Fig.11 and 12), is the limit of the converter operation in Z.C.S. mode. The discontinuous conduction mode is represented by the dotted curves.

CONCLUSION

The analytical study presented in this paper shows that the resonant converter in the Z.C.S. mode also presents some characteristics that depend strongly on the choice of the parameters, when the snubbers are not neglected. This study is even more valid when the chopped frequency increase, because the value of the snubber inductors of the inverter and the snubber capacitors of the rectifier are not negligible compared with those of the resonant circuit LC. Thereby, this plotting characteristics software arised from the analytical study constitutes a good tool in analysing the converter operation, but also a powerful tool to design the converter. This software connected with a simulation software such as S.U.C.C.E.S.S.[7 - 8] allows plotting the converter wave-forms in steady state.

REFERENCES

1) Chéron Y.,1992, "Soft commutation", Chapman & Hall, London (U.K.).

2) Vorperian V. And Cuk S., 1986, IEEE Industry Application, 640-647.

3) Oruganty R.L. And Lee F. C., 1984, IEEE Industry Application, 860-867.

4) Lee C. Q. And Siri K., 1986, IEEE Trans. on AES, 537-544.

5) Kuo-peng P., Chéron Y. And Cussac Ph., 1991, EPE'91 Florence, 4, 231-237.

6) Roudet J., 1990, " Analyse et comparaison des divers modes de conversion statique CC-CC. Mode de commutation et sureté de fonctionnement - Performances C.E.M.". Thèse INP Grenoble (France).

7) Piquet H., 1990, " Simulation numérique des convertisseurs statiques : prise en compte des boucles de contrôle ". Thèse INP Toulouse (France).

8) User's guide of S.U.C.C.E.S.S., 1992, CIRTEM. Toulouse (France).

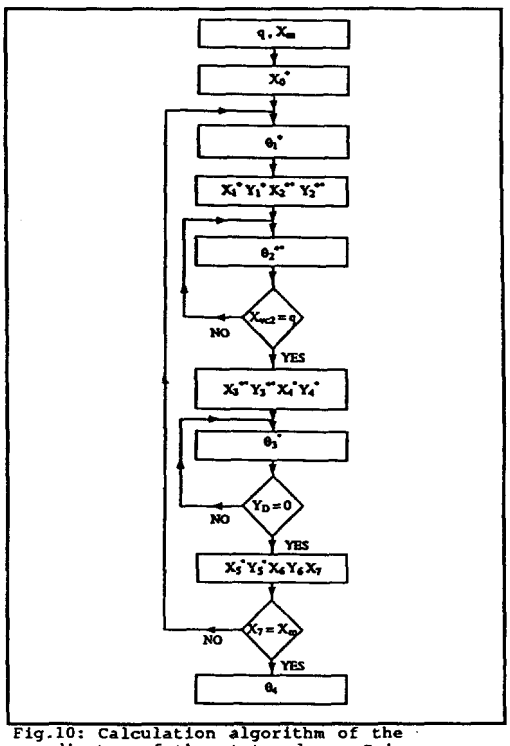

Fig.10: Calculation algorithm of the coordinates of the state plane. Criss-cross operation

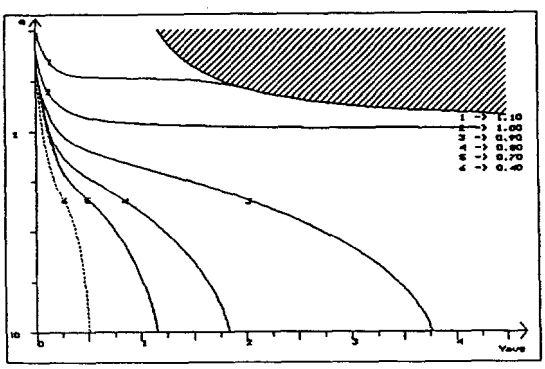

Fig.11: Output voltage versus average load current at a constant frequency. a_1 = 0.1 and a_2 = 0.5

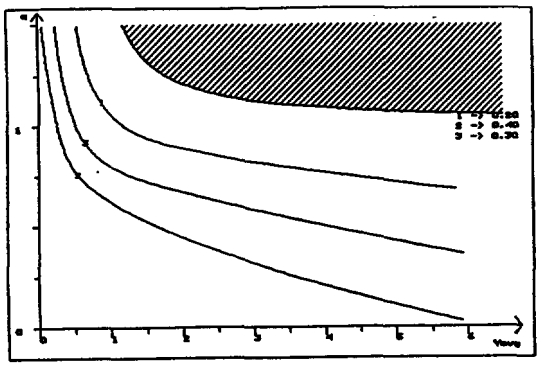

Fig.12: Output voltage versus average load current at a constant delay angle. a_ℓ = 0.1 and a_2 = 0.5

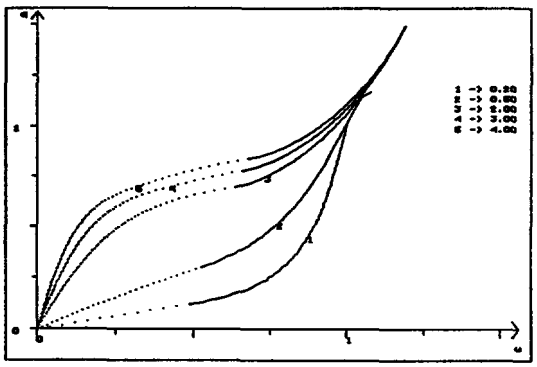

Fig.13: Output voltage versus frequency control with fixed load. a_ℓ = 0.1 and a_2 = 0.5

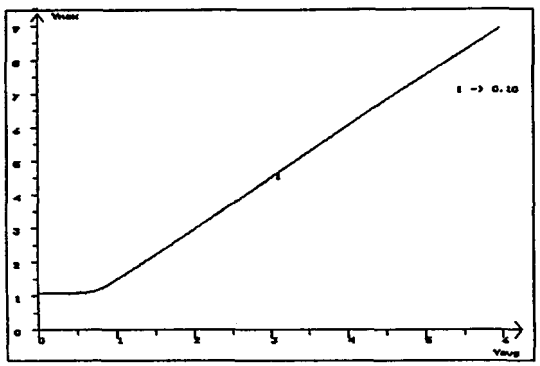

Fig.14: Peak current in the resonant tank versus average load current at a constant output voltage. a_ℓ = 0.1 and a_2 = 0.5